

Imperfections in amorphous chalcogenides.

I. Electrically neutral defects in liquid sulfur and arsenic sulfides

H. Kawazoe, H. Yanagita,* Y. Watanabe, and M. Yamane

Department of Inorganic Materials, Tokyo Institute of Technology, Ohokayama, Meguro-ku, Tokyo 152, Japan

(Received 6 July 1987; revised manuscript received 2 November 1987)

The structures of chain ends in liquid S, As-S, and As-Ge-S were examined by use of ESR. They were found to be composed exclusively of radical species with electrically neutral dangling bonds. This means that formation of positively or negatively charged species is less probable in the liquids. The temperature dependence of the concentration of radical species followed the Arrhenius law, thus suggesting the existence of chemical equilibria between the normal bonding state and the dissociated states. S—S and As—As homopolar bonds were also detected by resonance Raman scattering even in the stoichiometric As₂S₃ glass. These facts were interpreted in the following way: The initial reaction of bond fission in the liquids is thought to be radical cleavage of a normal bond. In the case of binary systems radical terminating reactions between the initial species give rise to the formation of homopolar bonds. Because of small enthalpy difference between the normal bond and the homopolar bonds, the concentration of homopolar bonds is expected to be high, which is consistent with the experimental observations.

I. INTRODUCTION

Structural imperfections in amorphous materials have been known to play a significant role in their optical and electrical properties. The imperfections in network glasses are tentatively defined as any deviation from an ideal random network or from chemically standard bonds expected from chemical composition. A dangling bond on a Si atom in deposited *a*-Si is a typical example of a localized level of high concentration in the band gap. It is "well known" that the concentration of the dangling bonds is greatly reduced by hydrogenation, and that the doping technique devised for crystalline semiconductors is applicable to *a*-Si:H.¹

The presence of the structural imperfections and defects in plate glasses and cups has attracted less attention than in the case of chalcogenide glasses. Glass products are usually manufactured from natural raw materials with a wide variety of impurities. These may conceal the effects of the imperfections on the properties. Another reason may be that weak ionic bonding between —O⁻ (nonbridging oxygen) and network-modifying cations such as alkali-metal ions breaks at lower temperatures than the covalent bonds in the network and disturbs the formation of bond defects in the melts. However, recent studies on transmission loss of silica-based optical waveguides due to color centers and —OH groups formed under the reaction of some structural defects with H₂ molecules diffusing from atmosphere² clearly showed the importance of the imperfections even in oxide glasses when they are of high purity. In a preceding paper,³ we proposed structural models of a drawing- or radiation-induced defect associated with Ge in SiO₂:GeO₂ fibers based on detailed analysis of their ESR absorptions. A series of chemical reactions in TO₂ melts (*T*=Si or Ge) was proposed as the mechanism for forming the drawing

induced defects. The net reaction is shown as $2TO_2 \leftrightarrow 2TO + O_2$, which gives rise to the reduction of *T* IV to *T* II. This is the thermal decomposition of the glass network into diatomic and highly volatile molecules. The initial reaction is the radical cleavage of the $\equiv T-O$ bond forming $\equiv T \cdot$ (*E'* center or T_3^0) and $\cdot O-(OHC$ or $C_{(1)}^0$) radicals, which are electrically neutral defects. Here the notation proposed by Kastner *et al.*⁴ is used: *T* is the element belonging to the fourth group of the Periodic Table and *C* denotes chalcogen atoms. The Superscript and subscript represent charge state and coordination number, respectively. Some other imperfections such as —O—O—, *T*—*T*, Ge²⁺, all experimentally detected or suggested to be present, are explained as the secondary products formed under the reactions among the initial radical species. Another factor affecting the formation of defects is the quenching rate of the melts, which determines the temperature at which the equilibria of the reactions are frozen.

These findings are exciting because even in ionic or polar oxides radical cleavage giving rise to electrically neutral defects occurs to an experimentally detectable extent ($\sim 10^{16}/g$). Chalcogenide glasses are the second example in which electronic defects control substantially their optical and electrical properties. The structural identity of the defects is still a matter of controversy, although the electrically charged defect model proposed by Anderson⁵, Mott, Street, and Davis⁶ and Kastner, Adler, and Fritzsche⁴ has been used in the explanations of the properties. The basic, main, or starting assumption of the theory is that a pair of a positively and negatively charged defects is energetically more favorable than two electrically neutral defects as the fission products in the chalcogenide network (so-called negative *U*) because of lattice distortion which compensates the repulsion energy between two electrons on a negatively charged ion. The

band model of amorphous chalcogenides involving the charged defects well explains a wide variety of optical and electronic phenomena. However, as far as we are aware, there has been no direct experimental evidence that supports the presence of charged defects.

When considering the fact that electrically neutral defects were detected even in ionic oxides, neutral defects in chalcogenide systems seem to be underestimated; neutral defects of higher concentration are to be present in more covalent chalcogenides. In addition, the formation of homopolar bonds (or wrong bonds) in binary chalcogenides is understandable as a natural consequence because the bonds are the products of radical termination reactions. The concentration of the bonds is of the order of $10^{19}/\text{g}$,⁷ and surprisingly enough, the mechanism of their formation was not interpreted reasonably well.

It is, therefore, very important to examine systematically what kinds of defects really exist in chalcogenide melts at a particular temperature and how these defects recombine to form normal bonds or homopolar bonds under a cooling process. In a present paper we report the formation of singly occupied dangling bonds in liquid sulfur at temperatures higher than those examined in an extensive work by Gardner and Frankel.⁸ Formation of radical species in As_2S_3 melts are also examined first as a function of temperature. Detection of homopolar bonds by resonance Raman scattering is stated, which is an indication of radical decompositions in liquid chalcogenides. In subsequent papers^{9,10} the detection of neutral defects in Ge-As-S glasses, the results of their structure analysis, and discussions about the mechanism for their formation will be given. Also the results of energy-band calculations on an alternate model of the gap states in chalcogenide glasses will be reported, which is newly proposed and named "interacting-lone-pair model."

II. EXPERIMENT

A. Sample preparation

As and S of 99.999% purity were used as raw materials. Sulfur atoms were further purified once by sublimation to remove organic contaminants. The oxidized layer on the surface of As was also removed by heating at 350 °C under vacuum. In preparing As-S glasses ($\text{As}_{40}\text{S}_{60}$, $\text{As}_{42}\text{S}_{58}$, and $\text{As}_{38}\text{S}_{62}$), theoretical amounts of the purified S and As were weighed and sealed into a silica ampoule under vacuum. Total weight was about 5 g. They were first melted with a rocking furnace at $\sim 700\text{--}800^\circ\text{C}$ for 24 h to homogenize, then kept at an appropriate temperature ($\sim 400\text{--}650^\circ\text{C}$), and finally air or water quenched. A small amount (0.05–0.1 g) of the sulfide glass was sealed under vacuum into another silica tube 3 cm long with an inside diameter of ~ 2 mm for ESR measurements at high temperature.

B. ESR measurements

For high-temperature measurements a platinum resistance heater was made by painting Pt paste in a shape of two thin strips 1 mm wide and 6 cm long along opposite

sides of a fused silica tube which was heated at about 800 °C. The heater was inserted into a vacuum double tube of silica glass for thermal insulation. A silica ampoule was placed in the center of the heating tube. Background absorption due to a heater element and reduction of sensitivity were pronounced at high temperature. The temperature was measured by a platinum-rhodium thermocouple inserted into the thermal insulation tube from its bottom up to just inside of a cavity. The temperature difference between the center of a cavity and the measured position was calibrated before the ESR measurements. The intensity of the ESR signal was calibrated by comparing with the stable absorption due to Cu^{2+} or Cr^{3+} in the aluminosilicate glass with high softening point ($\sim 900^\circ\text{C}$). Temperature of the measurements was from room temperature to $\sim 700^\circ\text{C}$. The ESR was measured on a JEOL FE-2XG instrument equipped with a TE_{011} mode cavity. The operating microwave power was suppressed to less than 0.1 mW to avoid saturation. The magnetic field and microwave frequency were calibrated using a proton NMR marker and a cavity wave meter, respectively.

C. Raman scattering and optical measurements

Raman scattering from the chalcogenide samples was measured at room temperature using He-Ne (633 nm) and Ar-ion (514.5, 502, 488, 497, and 476 nm) lasers. The optical power output from the Ar-ion laser was usually on the order of milliwatts to minimize damage to the samples. The scattered light was focused by a lens onto the slit of a $\frac{1}{4}$ -m double monochromator. Polarization measurements were not done.

The optical absorption was measured to estimate the optical band gap by using a laboratory-made photoacoustic spectrometer, which consists of a Xe lamp, monochromator with 10 cm length for the light source, chopper, and sample cell with a microphone detector. The output of the microphone was amplified by a lock-in amplifier. The measurements were done on powdered samples at room temperature. The intensity of the photoacoustic signal from a sample for respective wavelength was normalized by dividing with the corresponding output from carbon.

III. RESULTS AND DISCUSSION

A. Radical species in liquid sulfur

Figure 1 shows X-band ESR absorptions of liquid sulfur observed at high temperature. The broad absorption, which is denoted by dashed lines and intense at high temperature, is a background absorption due to the Pt heater. Three characteristics are notable in the figure. The first is the appearance of a Zeeman resonance with $g = 2.024$ at temperatures higher than 160 °C. (This is the temperature for which viscosity goes up stepwise.) The resonance has been assigned to a sulfur atom radical, $-\text{S}\cdot$.⁸ This suggests that S_8 ring molecules contained in liquid S begin to break, forming long linear chains.¹¹ The

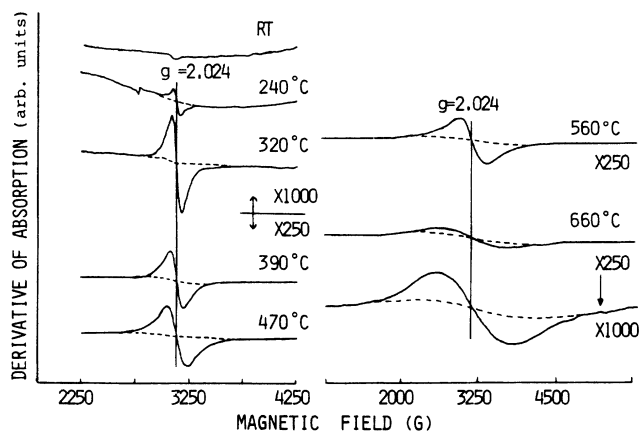


FIG. 1. X-band (8.91 GHz) ESR spectra of liquid sulfur. Temperature ($^{\circ}\text{C}$) of measurements and amplifier gain are given in the figure. Dashed lines denote background absorption due to a Pt heater element.

second is its line shape and linewidth. The line shape was found to be almost Lorentzian, which is characteristic of the homogeneously broadened absorption due to spins in liquids, and the width increased markedly with increasing temperature. This would be due to the decrease in lifetime of the radical species which occurs in turn by chemical exchange, spin-lattice, or spin-spin relaxation.

The third characteristic is the fact that concentration of the radical species is very high especially at higher temperatures. The concentration of radical species was estimated by twice integrating the derivative spectra and comparing the estimated area with that of the known amount of Cu^{2+} dissolved in the aluminosilicate glass standard. The equilibrium concentration of radical species was plotted in Fig. 2 as a function of temperature. The dashed line is a similar plot reported by Gardner *et al.*⁸ The discrepancy between these two lines may originate from the difference in temperature measurements. A single and straight line with a slope of $\Delta H = 33$

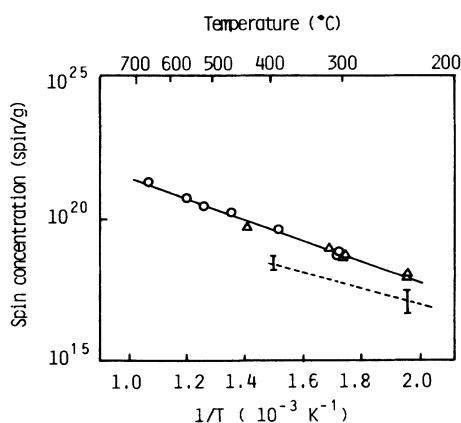


FIG. 2. Temperature dependence of spin concentration per unit mass of liquid sulfur (solid line). The dashed line is the data of Ref. 8.

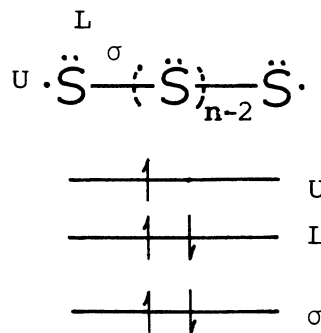


FIG. 3. Structure and electronic structure of chain ends of radical chains in liquid sulfur. σ , L , and U mean a σ bond between two sulfur atoms, a lone-pair electron on a sulfur atom, and an unpaired electron on the terminal sulfur atom, respectively. n denotes number for degree of average polymerization of a radical chain.

kcal/mol was obtained. This is in close agreement with those reported by Gardner *et al.* and by Gee¹² from thermodynamic properties. The absolute concentration of spins at 700°C was $\sim 1.3 \times 10^{21}$ spin/g, which was equivalent to ~ 3.5 mol %. This value is consistent with that estimated by magnetic susceptibility measurements.¹³ It is interesting to note that the average chain length (polymerization degree) of ~ 50 at the temperature, which was obtained by viscosity measurements,¹⁴ is in close agreement with the spin concentration if the chain ends are exclusively composed of a sulfur atom radical. This implies that at least several (10%) of the chain ends are neutral defects. Electronic structure of the defect species is given in Fig. 3 schematically. Each S atom at the chain end is carrying one unpaired electron. This means that on an average four electrons are on each sulfur atom, which suggests the sulfur atoms on chain ends are in an electrically neutral state. Schematic electronic configuration is also given in the figure, where $3s^2$ electrons were excluded from the present discussion because of their far lower energy compared with those for $3p$ electrons of S atoms.

From these results chemical reactions involved in the melting of crystalline and liquid sulfur can be summarized in the following: At the melting point (120°C) crystalline S changes into a molecular liquid of S_8 rings. There is an equilibrium of thermal and homolytical dissociation of S_8 rings above the temperature. The bond breaking reaches a detectable amount of 160°C . In this stage liquid S is composed of long linear radical chains and the viscosity increases abruptly.¹⁴ The conversion of S_8 rings to a long linear chain seems to be favored at higher temperatures. At $\sim 700^{\circ}\text{C}$ all molecules are likely to be changed to linear radical chains with an average chain length of ~ 50 .

B. Radical species in liquid As_2S_3

High-temperature ESR measurements similar to those done for liquid sulfur were also carried out for liquid

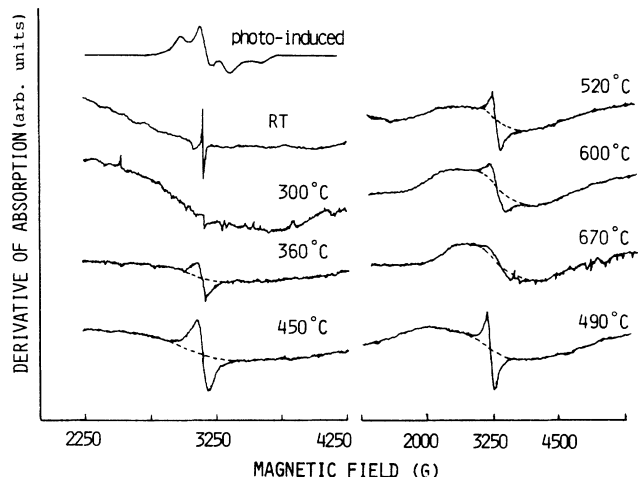


FIG. 4. X-band (8.91 GHz) ESR spectra of liquid As_2S_3 . Temperature ($^{\circ}\text{C}$) of measurements is shown in the figure. The upperleft signal was obtained by illuminating the glass with band-gap light at 77 K. Background absorption was pronounced at high temperatures, which is due to a Pt heater element.

As_2S_3 and the results are shown in Fig. 4. Dashed lines show a background absorption due to a Pt heater. Again in this case broad absorption without any hyperfine structure, similar to those observed for liquid sulfur was detected at above 360°C . The sharp absorption seen around 3200 G at RT disappeared at 300°C and was not detected on farther cooling of the sample. Although conclusive assignment of the absorption has not been given, this is suggested to be due to carbon impurity.¹⁵ We confine ourselves to the broad and stronger absorptions. The line shape changed from Lorentzian to Gaussian at about 500°C with increasing temperature. This shows a large difference between the responses of radical species in liquid S and liquid As_2S_3 .

The spin concentration of radical species in liquid As_2S_3 is plotted as a function of reciprocal temperature in Fig. 5. A straight line was obtained, which suggests that

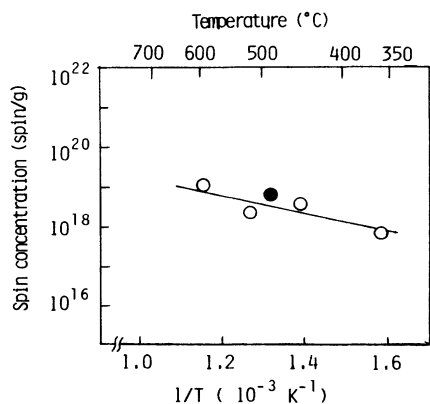


FIG. 5. Temperature dependence of spin concentration per unit mass of liquid As_2S_3 .

there is an equilibrium concentration of radical species in the melt. Because of the large linewidth of absorptions especially at a higher temperature, there were some difficulties in determining spin concentration. However, the slope, which expresses an enthalpy difference between the normal bonding state of As-S and some state involving radical species, was estimated to be $\sim 14 \pm 3$ kcal/mol, which is considerably lower than the bond energy of As-S , 31 kcal/mol. The apparent discrepancy between the enthalpies will be explained after identifying the radical species in the following subsection.

C. Identification of the radical species in liquid As_2S_3

There was considerable difficulty in identifying the radical species detected in liquid since the ESR absorptions were a broad resonance without hyperfine structure (Fig. 4). We, however, think that the signal includes the absorptions of As-related radicals as well as that of S based on the following observations.

If As-S bonds in the liquid dissociate homolytically, sulfur- and arsenic-related radicals must be detected. In the case where unpaired spin localizes on an As atom in a solid matrix, it gives rise to the absorption similar to that shown in the upperleft corner of Fig. 4, which was obtained by illuminating As_2S_3 glass with band-gap light at 77 K. The structure analysis of a center responsible for the absorption will be discussed in detail in the subsequent paper.⁹ The structure has been shown to be an arsenic atom doubly coordinated by two sulfur atoms, and carrying one lone pair of electrons and one unpaired electron that has totally localized on the $3p$ atomic orbital of the central arsenic atom. This is designated as $=\text{As}:$ or $P_{(2)}^0$, where P , its superscript, and subscript mean pnictide, charged state, and coordination number, respectively. The complex features of the spectrum originate from anisotropic g and hyperfine tensors, the latter denoting the interaction between the unpaired electron and ^{75}As nucleus ($I = \frac{3}{2}$ and 100% natural abundance). There is an indication of line broadening due to hyperfine interactions caused by more distant ^{75}As nuclei because the linewidth of the absorption due to a similar center in the glasses in which concentration of arsenic is much less than As_2S_3 is considerably narrower than that for As_2S_3 glass.⁹

The important point in the present discussion is how the lineshape characterized by an anisotropic hyperfine interaction of ^{75}As changes on going from solid to liquid state. In order to examine the smearing out process of hyperfine structure on liquidization, ESR of glassy and liquid $30\text{GeS}_{1.5} \cdot 5\text{As}_2\text{S}_3$ was measured. For this composition we could first observe formation of As-related and electrically neutral radicals even in a glassy state. Figure 6 exhibits the spectra measured at different temperatures. The signal obtained at room temperature implies the simultaneous formation of an unpaired spin localizing on As or Ge in the quenched glass. Upon heating the glass the unpaired spins were thermally bleached out at about 340°C , but reappeared at higher temperatures. There are two interesting characteristics in the figure. One is the change in line shape with increasing temperature. Another

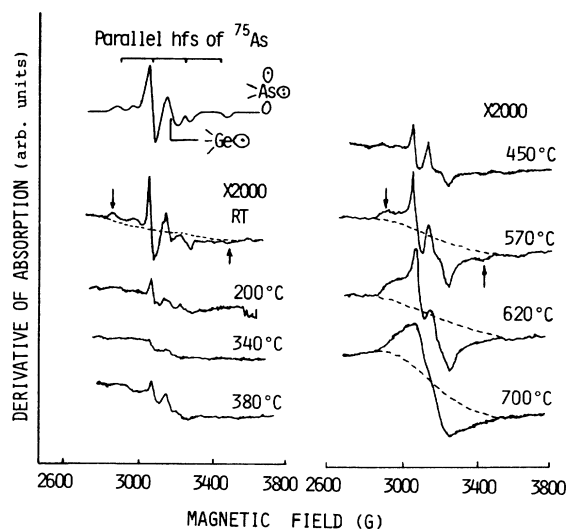


FIG. 6. X-band (8.92 GHz) ESR spectra of 30 GeS_{1.5}·5 As₂S₃ melts. The upper left-hand trace is a calculated spectrum for =As: (P_2^0) + Ge $E'(T_3^0)$ center. Temperature (°C) of measurements and amplifier gain are given in the figure. Arrows show the lowermost and uppermost hyperfine shoulders due to ⁷⁵As nucleus.

er is the large increase in absorption intensity on going from a low to high temperature above 340°C. The splitting between the uppermost and lowermost hyperfine shoulders (shown by arrows in the figure) of the spectrum is a good measure of rotational diffusion rate of the paramagnetic species.¹⁶ It decreases with increasing temperature, suggesting fast molecular motion at high temperature. It is noted that the sharp features were lost at 700°C and the line shape changed to Gaussian, which is a characteristic of the absorption inhomogeneously

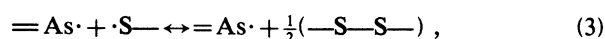
broadened by hyperfine interactions. The line shape originates from implicit hyperfine structure due to ⁷⁵As nucleus because there are no nuclei other than ⁷⁵As having nonzero nuclear spin in the system. Since the line shape of As₂S₃ melt at high temperature was found to be Gaussian it is highly probable that As-related radicals are present in the melt especially at higher temperature.

D. Chemical equilibria associated with bond dissociation in liquid As₂S₃

In this subsection we discuss the apparent discrepancy between the enthalpies of dissociation of As—S bonding and that obtained from the slope of Fig. 5. The apparent inconsistency can be explained by assuming the existence of several competing reactions between the radical species formed on the thermal decomposition of As—S bonds at high temperature. The initial reaction is thought to be



Secondary reactions between the initial products are naturally expected for the binary systems



and



These are likely to be regarded as the ground state (=As—S—) and chemically excited states: The products in the right-hand side of Eqs. (1)–(4) and the normal bonds (=As—S—) are in chemical equilibrium with each other via the dissociated state (=As· + ·S—). Therefore, we can reasonably assume chemical equilibria among these five states. An equilibrium and total concentration of the radical species are given by

$$[As\cdot] + [S\cdot] = \frac{2 \exp(-\Delta H_1/RT) + \exp(-\Delta H_2/RT) + \exp(-\Delta H_3/RT)}{1 + \exp(-\Delta H_1/RT) + \exp(-\Delta H_2/RT) + \exp(-\Delta H_3/RT) + \exp(-\Delta H_4/RT)} \quad (5)$$

where ΔH_i 's are enthalpy difference between the ground and excited states and R is the gas constant. A rough estimate of Eq. (5) is easily obtained. The exponential terms in the denominator are considerably smaller than unity, thus the denominator is approximated to be ~ 1 for the temperature region under discussion. The dominating term in the numerator is that with the smallest ΔH_i . Keeping only the dominant term, we can rewrite Eq. (5) as

$$\log_{10}\{[As\cdot] + [S\cdot]\} = \text{const} - 0.4343\Delta H_i/RT \quad (6)$$

This expression explains the observed facts well: the linear relation between $1/T$ and the log of the spin con-

centration, and the unexpectedly low slope of the plot. The former is apparent from the shape of Eq. (6) and the latter is the result of approximating the reaction with the lowest ΔH_i which represents the formation of the radical species, As· or S·. Therefore, the apparent slope is to be viewed as the enthalpy change associated with reaction (2) or (3). At the moment we cannot decide which reaction is dominant in the formation of the radical species. However, the fact that the line shape changed from Lorentzian to Gaussian may suggest that ΔH_2 is much larger than ΔH_3 , which predicts the increase in concentration of =As: at high temperature.

Apparently the low spin concentration of liquid As₂S₃

compared with liquid S is considered to be partly due to low bond density per unit mass (half of that of liquid S) and presence of the homopolar bonds in the binary system.

E. Resonance Raman scattering of As-S glasses

Simultaneous formation of homopolar bonds was suggested in the explanation of the formation of radical species in liquid As-S. Equilibrium concentration of the bonds is surprisingly high because of low enthalpy difference between the homopolar bonds and normal As—S bonds. Therefore, the homopolar bonds are expected to remain in the glass produced by quenching the melt. Resonance Raman scattering is an appropriate technique for detecting chemical species of low concentration.^{17,18} Figure 7 shows optical-absorption spectra of the powdered arsenic sulfides measured by using photoacoustic spectroscopy. As was reported by preceding papers, the band edge showed pronounced blue shift with increasing S content. The arrows on the bottom exhibit wavelengths of emissions from Ar-ion laser and He-Ne laser, which were used as an excitation source of Raman scattering. Figure 8 denotes reduced Raman scattering spectra of As_2S_3 glasses obtained by using different excitation light. Since optical absorption at 633 nm is slight, the spectrum obtained by using He-Ne laser is considered to be nonresonant Raman scattering. This is identical with those reported in the literature.^{19,20} Other spectra in the figure are measured by using excitation light with wavelength within absorption bands. We can see little change among the spectra, while clear changes are noted on going from the excitation wavelength of 633 to 514.5 nm. Relative intensity of the bands at 230 and 490 cm^{-1} with respect to the strong peak at 340 cm^{-1} increased considerably, when excited by the lights with wavelength within the optical-absorption band. The former is assigned to As—As homopolar bonds²¹ and the latter to S—S homopolar bonds.²² Thus the simultaneous forma-

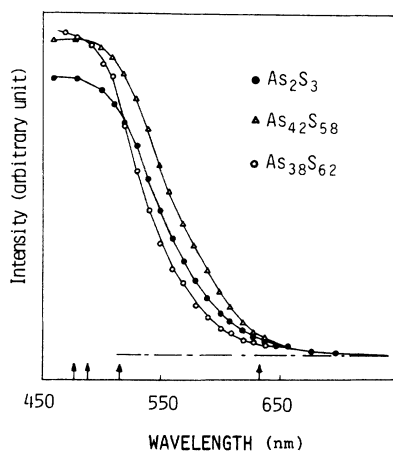


FIG. 7. Photoacoustic spectra of As-S glasses. Arrows in the bottom exhibit wavelengths of the emission from He-Ne or Ar-ion laser used for excitation.

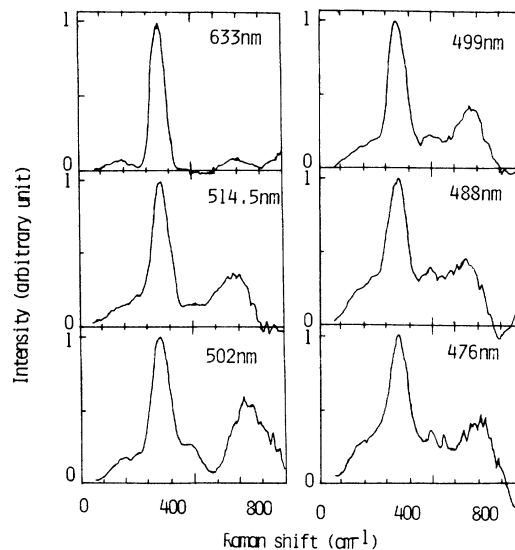


FIG. 8. Reduced Raman spectra of As_2S_3 glasses quenched from 650°C. Wavelength of the excitations is shown in the figure. Signal intensity was normalized relative to the intense 340 cm^{-1} band having an intensity of 1. Measurements were carried out at room temperature.

tion of As—As and S—S homopolar bonds in As_2S_3 glass was firmly established.

IV. CONCLUDING REMARKS

In the present study nature of chain ends in liquid S, As-S and As-Ge-S was clearly shown by measuring directly ESR of the liquids at high temperature. In the chalcogenide liquids chain ends were found to be exclusively composed of free radicals, electrically neutral, and singly occupied dangling bonds; this means that formation of charged defects in the liquids is less probable. In the case of binary and ternary systems, the radical terminating reactions must be taken into account, which give rise to the formation of homopolar bonds. Formation of homopolar bonds even in the stoichiometric As_2S_3 glass was experimentally evidenced by using resonance Raman scattering. It was suggested that there are chemical equilibria between normal bonds, which can be regarded as the thermal ground state, and thermally excited states, broken bonds, and homopolar bonds. It was stressed that the concept of hierarchy in bond strength in a liquid is very important as a factor controlling the liquid structure. In the case of S there is a successive cleavage of weak intermolecular interaction between S_8 molecules and strong intramolecular bonds on going from low to high temperature. Therefore the low-temperature liquid is viewed as a molecular liquid and that of high temperature is a liquid of radical species.

ACKNOWLEDGMENTS

This work was in part supported by a Grant-in-Aid for Scientific Research from the Ministry of Education, Science, and Culture Grant No. 60 470 070.

- *Present address: HOYA Corporation Miyazawa-cho, Akishima-shi, Tokyo 196.
- ¹W. E. Spear and P. G. Le Comber, *Solid State Commun.* **17**, 1193 (1975).
- ²T. Tanifuji, M. Matsumoto, M. Tokuda, and M. Miyauchi, *Electron Lett.* **20**, 13 (1984).
- ³Y. Watanabe, H. Kawazoe, K. Shibuya, and K. Muta, *Jpn. J. Appl. Phys.* **25**, 42 (1986).
- ⁴M. Kastner, D. Adler, and H. Fritzsche, *Phys. Rev. Lett.* **37**, 1504 (1976); M. Kastner and H. Fritzsche, *Philos. Mag.* **37**, 199 (1978).
- ⁵P. W. Anderson, *Phys. Rev. Lett.* **34**, 953 (1975).
- ⁶R. A. Street and N. F. Mott, *Phys. Rev. Lett.* **35**, 1293 (1975); N. F. Mott, E. A. Davis, and R. A. Street, *Philos. Mag.* **32**, 961 (1975).
- ⁷P. Boolchand, in *Physical Properties of Amorphous Materials*, edited by D. Adler, B. B. Schwartz, and M. C. Steele (Plenum, New York, 1985), p. 221; *Mater. Res. Soc. Symp. Proc.* **61**, 57 (1986).
- ⁸D. M. Gardner and G. K. Fraenkel, *J. Am. Chem. Soc.* **78**, 3279 (1956).
- ⁹Y. Watanabe, H. Kawazoe, and M. Yamane, following paper, *Phys. Rev. B* **38**, 5668 (1988).
- ¹⁰Y. Watanabe, H. Kawazoe, and M. Yamane, this issue, *Phys. Rev. B* **38**, 5677 (1988).
- ¹¹F. A. Cotton and G. Wilkinson, *Advanced Inorganic Chemistry, A Comprehensive Textbook*, 4th ed. (Wiley, New York), p. 508.
- ¹²G. Gee, *Trans. Faraday Soc.* **48**, 515 (1952).
- ¹³*Elemental Sulfur Chemistry and Physics*, edited by B. Meyer (Interscience, New York, 1965).
- ¹⁴Bacon and Fanelli *J. Am. Chem. Soc.* **65**, 539 (1943).
- ¹⁵M. H. Brodsky and R. S. Title, *Phys. Rev. Lett.* **23**, 581 (1969).
- ¹⁶A. Abragam, *The Principles of Nuclear Magnetism* (Oxford, New York, 1961).
- ¹⁷G. Carini, M. Cutroni, M. P. Fontana, G. Galli, and P. Migliardo, *Solid State Commun.* **23**, 1143 (1980).
- ¹⁸P. J. S. Ewen and A. E. Owen, *J. Non-Cryst. Solids* **35/36**, 1191 (1980).
- ¹⁹S. A. Solin and G. N. Papatheodorou, *Phys. Rev. B* **15**, 2084 (1977).
- ²⁰R. J. Nemanich, G. A. N. Connell, T. M. Hayes, and R. A. Street, *Phys. Rev. B* **18**, 6900 (1978).
- ²¹R. J. Kobliska and S. A. Solin, *J. Non-Cryst. Solids* **8-10**, 191 (1972).
- ²²R. J. Kobliska and S. A. Solin, *Phys. Rev. B* **8**, 756 (1973).